Science and Engineering Research Council
Rutherford Appleton Laboratory
CHILTON, DIDCOT, OXON, OX11 0QX

RAL-86-041

The Determination of the Complete Neutron Scattering Law S(k,w) from Total Scattering Experiments using Computed Tomography.

M.W. Johnson

May 1986

The Determination of the Complete Neutron Scattering Law $S(\kappa,\omega)$ from Total Scattering Experiments using Computed Tomography.

M W JOHNSON

Rutherford Appleton Laboratory
Chilton,Oxon,OX11 0QX

ABSTRACT

This paper describes how the considerable body of knowledge on image reconstruction from path integrals (computed tomography) may be applied to total, time-of-flight neutron scattering experiments (ie those involving no experimental energy analysis) to obtain the neutron scattering law $s(\kappa,\omega)$. We examine the feasibility in terms of possible instrument geometries and reconstruction algorithms . It is possible that such reconstruction techniques may have wide application in the fields of neutron powder diffraction, amorphous scattering, liquids scattering and quasi-elastic incoherent scattering.

A simple algorithm is presented which enables the tomographic problem with curved path integrals to be solved.

1 INTRODUCTION

In a time-of-flight neutron scattering experiment in which no energy analysis is perfomed the recorded intensity in a particular detector and time channel is related to a curved path integral over the κ,ω plane. Adjacent time channels from the same detector provide an integral over a neighbouring,parallel,curved path. Typical paths for a detector at a scattering angle (2Θ) of 5^{o} are shown in Fig.1a . Detectors at different scattering angles have different paths and those for 10^{o},20^{o} and 30^{o} are shown in Fig.1b,c and d.

If the path integral can be written down in terms of a scattering law which is path-independant the problem may be mapped to the image reconstruction problem solved in real-space tomography.

In section 2 we establish an algorithm for the solution of a tomographic problem with curved path integrals.

In section 3 we show how a total-scattering time-of-flight experiment may be expressed in a form suitable for reconstruction.

Section 4 presents some preliminary results which show how quite remarkable resolution would appear to be possible using the technique.

Section 5 indicates some of the problems which remain to be solved and gives some preliminary definitions of the instrument design required to maximise the potential of this technique.

2 TOMOGRAPHY

Computed Tomography has been applied in radiology and electron microscopy for many years, and a review of the algorithms used has been published by Gordon and Herman [1] . For use with curved path integrals the ART (Algebraic Reconstruction Technique [2,3]) algorithm is particularly suitable and has a simple intuitive basis.

The object to be considered will be represented by a rectangular array of n x m cells each with a density ρ_{ij} . This is shown in Fig.2 below.

A path integral P_k may be defined by the sum,

$$P_k = \sum_{i,j \subset path} \rho_{ij}\lambda_{ijk} \qquad - 2.1$$

where the sum is taken over all i,j contributing to the path and λ_{ijk} is the curved path length in cell (i,j) for path k.

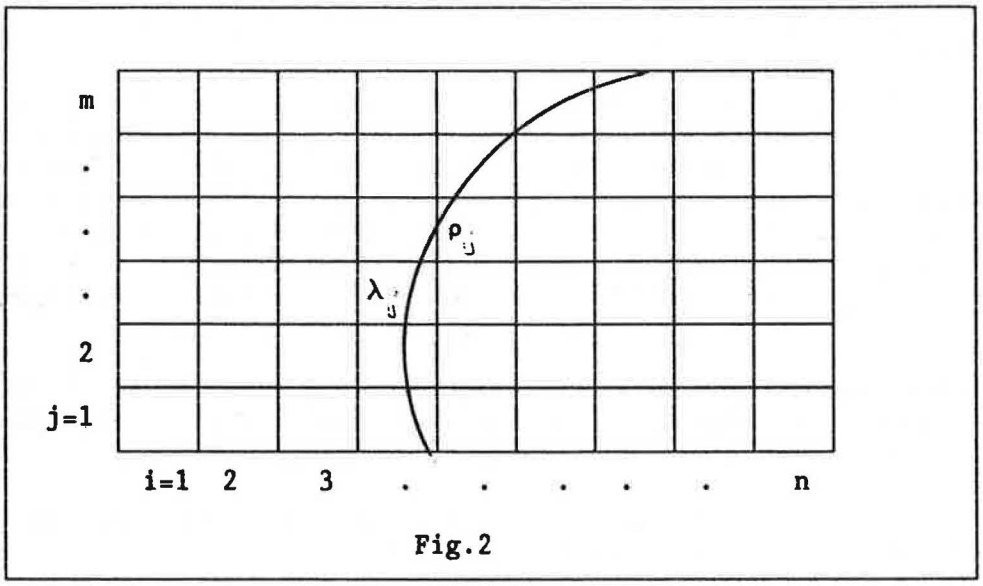

Fig.2

Clearly the summation may be trivially extended over all i,j since

$$\lambda_{ijk} = 0 \qquad - 2.2$$

for cells not contributing to the path. Thus:

$$P_k = \sum_{i,j} \rho_{ij}\lambda_{ijk} \qquad - 2.3$$

Tomography consists in solving the inverse problem in which P_k and λ_{ijk} are the known quantities and ρ_{ij} are the unobserved,desired quantities.

The multiplicative ART algorithm consists of the following steps:

1. Define an initial guess ζ_{ij} for all ρ_{ij}.

2. Select a path k.

3. Calculate an improved guess ζ'_{ij} to satisfy the observed path integral P_k by a multiplicative modification of the previous ζ_{ij}.

$$\zeta'_{ij} = \zeta_{ij}(1+\alpha\lambda_{ijk}) \qquad \text{for all } i,j \qquad - 2.4$$

Since we require

$$\sum_{i,j} \zeta'_{ij}\lambda_{ijk} = P_k \qquad - 2.5$$

then

$$\sum_{i,j} \zeta_{ij}(1+\alpha\lambda_{ijk})\lambda_{ijk} = P_k \qquad - 2.6$$

and

$$\alpha = \frac{P_k - \sum_{ij} \zeta_{ij}\lambda_{ijk}}{\sum_{ij} \zeta_{ij}\lambda^2_{ijk}} \qquad - 2.7$$

Repeated application of steps 2 and 3 lead to a representation ζ_{ij} for the desired quantities ρ_{ij} which is equivalent to the maximum entropy solution [5]. For the purposes of the demonstration of the technique we have chosen the total number of paths to equal the total number of cells nxm , and the path selection (step 2) is made at random.

3 TOTAL NEUTRON SCATTERING

We consider an idealised time-of-flight neutron scattering experiment in which a pulsed, white beam of neutrons is incident on a sample (S) and detected (D) at a scattering angle of 2Θ, Fig 3. All neutrons are assumed to leave the moderator (M) at time t=0 .

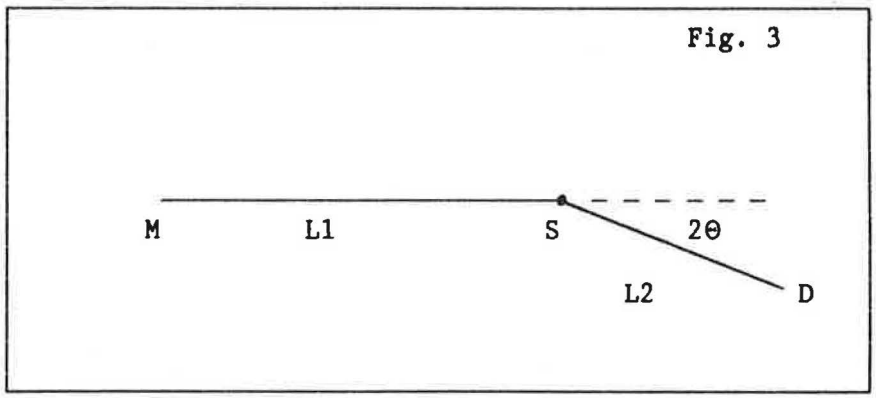

Fig. 3

Neutrons arriving at a time t at the detector may have been elastically or inelastically scattered , but their overall flight time t determines a relationship between their primary and secondary energies E1 and E2 .

We have

$$t = t1 + t2 = \frac{m}{\hbar}\left(\frac{L_1}{k_1} + \frac{L_2}{k_2}\right) = \sqrt{\frac{m}{2}}\left(\frac{L_1}{\sqrt{E_1}} + \frac{L_2}{\sqrt{E_2}}\right) \qquad - 3.1$$

Thus neutrons arriving at a particular time must have scattered from a point on a locus in the (E1,E2) plane defined by eq. 3.1.

More usefully we may describe this locus in the (κ,ω) plane where

$$h\omega = E_1 - E_2 \qquad - 3.2$$

$$\underline{\kappa} = \underline{k}_1 - \underline{k}_2 \qquad - 3.3$$

$$\kappa^2 = k_1^2 + k_2^2 - 2k_1k_2\cos(2\theta) \qquad - 3.4$$

For any value of E_2 , E_1 is defined (eq.3.1) and from these values $h\omega$ and κ may readily be determined (eqs. 3.2,3.4). The loci in the (κ,ω) plane are illustrated in Figs.1a-1d.

The point of selecting the (κ,ω) plane is that, as a consequence of the first Born approximation to the cross section [7], all neutron scattering cross sections may be described in the form

$$\frac{d^2\sigma}{d\Omega dE_2} = \frac{k_2}{k_1} F(\kappa,\omega)$$

where $F(\kappa,\omega)$ is a function only of κ,ω and not k_1 or k_2 . As an example a monatomic liquid has

$$F(\kappa,\omega) = \frac{N\sigma c}{4\pi} S(\kappa,\omega) \qquad - 3.6$$

Hence the number of neutrons arriving at a time t in the idealised experiment is proportional to

$$n(t) \propto \int_{E1,E2\ \text{locus}} \phi(E_1)\,\frac{d^2\sigma}{d\Omega dE_2}\,dE_2 \qquad - 3.7$$

$$n(t) \quad \alpha \quad \int_{\kappa,\omega \text{ locus}} \phi(E_1)\frac{k_2}{k_1} F(\kappa,\omega)\, dE_2 \qquad - 3.8$$

a path integral over the (κ,ω) plane. Writing eq.3.8 in a disrete form we have

$$n(t)_p \quad = \quad \sum w_{ijp} F_{ij} \qquad - 3.9$$

where Fij is the cross section in cell $\kappa_i \omega_j$ in the κ,ω plane and w_{ijp} is a weight for that cell ,for path p:

$$w_{ijp} = \phi(k_1)\frac{k_2}{k_1}\Delta E \qquad - 3.10$$

Since 3.10 is completely analagous to eq.2.3 with w_{ijp} taking the place of the path length within a cell it is possible to use the ART algorithm to solve eq.3.9 for F_{ij} when $n(t)_p$ and w_{ijp} are known.

4 AN EXAMPLE

To illustrate the possibilities of this method the following steps were followed.

The discrete scattering law F_{ij} shown in Fig.4 was set up. The ω channel boundaries were set to -40.0,-32.0,-24.0,-16.0,-8.0,-2.0, 2.0,8.0,16.0,24.0,32.0,40.0 (meV) and the κ boundaries at 4.0,4.01, 4.02,4.03....4.1 A-1.
Note that the ω channels were not all of the same size. The F_{ij} contained a 'Bragg peak' in channel (6,6) and was surrounded by much weaker 'inelastic' scattering.

Ten time of flight values were chosen for each of ten scattering angles and their corresponding loci in (κ,ω) space computed (see Fig.1). The t-values at each scattering angle were chosen to cross the near centre of each elastic channel. The scattering angles were $5,7.5,10,20,30,40,50,60,70,90^{o}$.

w_{ijp} were calculated for each path and the 100 path integrals computed from eq.3.9 ,3.10 with the assumption that the incident neutron spectrum, $\phi(E_1)$, was constant. The path integrals were then given random errors corresponding to fractional errors of ~ 0.5%.

The ART reconstruction algorithm was then applied with initial values

11	0.25	0.34	0.47	0.63	0.81	0.89	0.81	0.63	0.47	0.34
10	0.33	0.44	0.60	0.82	1.04	1.14	1.04	0.82	0.60	0.44
9	0.46	0.62	0.84	1.14	1.45	1.60	1.45	1.14	0.84	0.62
8	0.76	1.03	1.40	1.90	2.42	2.67	2.42	1.90	1.40	1.03
7	2.29	3.08	4.21	5.71	7.27	8.00	7.27	5.71	4.21	3.08
6	0.00	0.00	0.00	0.00	0.00	100.00	0.00	0.00	0.00	0.00
5	2.29	3.08	4.21	5.71	7.27	8.00	7.27	5.71	4.21	3.08
4	0.76	1.03	1.40	1.90	2.42	2.67	2.42	1.90	1.40	1.03
3	0.46	0.62	0.84	1.14	1.45	1.60	1.45	1.14	0.84	0.62
2	0.33	0.44	0.60	0.82	1.04	1.14	1.04	0.82	0.60	0.44
j=1	0.25	0.34	0.47	0.63	0.81	0.89	0.81	0.63	0.47	0.34
	i=1	2	3	4	5	6	7	8	9	10

Fig. 4

11	6.94	1.72	2.78	4.50	1.98	2.62	0.01	3.06	1.16	2.20
10	0.00	1.26	0.34	2.13	2.18	9.41	6.28	1.35	1.78	1.91
9	0.00	0.43	0.68	0.00	0.38	2.37	3.34	4.03	1.78	0.37
8	0.20	0.00	1.29	0.39	1.49	2.27	2.61	2.90	2.54	0.08
7	3.79	4.00	7.19	7.81	2.32	6.34	4.00	1.15	0.72	0.05
6	0.00	0.00	0.00	0.00	0.00	99.48	0.00	0.48	0.06	0.32
5	0.02	2.75	0.26	2.48	4.96	6.65	6.43	3.83	3.92	1.92
4	0.12	0.03	0.08	2.95	5.74	0.70	0.56	3.08	0.52	4.01
3	0.11	0.08	0.08	0.29	1.63	5.37	1.02	0.04	0.03	1.10
2	0.19	0.12	0.03	1.61	0.84	0.63	0.62	0.21	0.45	0.05
j=1	0.06	0.17	0.23	0.85	0.81	1.11	0.97	0.61	0.23	0.16
	i=1	2	3	4	5	6	7	8	9	10

Fig. 5

of G_{ij} (the guessed values of F_{ij}) all set to 0.01.

Fig.5 shows the reconstructed values after 9000 cycles . The 'R-factor' defined in eq.4.1 had reached 0.8% and the fractional error in the determination of the 'elastic component' (ie between -2.0 and 2.0 meV) was 2.3%.

$$\text{R-factor} = \frac{\sum (G_{ij} - F_{ij})^2}{\sum F_{ij}^2}$$

5 CONCLUSIONS

It is possible that the method described above may be of considerable use in separating elastic from quasi-elastic or inelastic scattering in neutron powder diffraction. If the κ-range accessible to many detectors is sufficiently large the technique may be extended to liquids and amorphous problems and possibly the mapping of quasi-elastic incoherent cross sections.

It should be emphasised that, while the simulation described in section 4 has included a number of realistic experimental parameters to demonstrate the potential of the method, it has ignored the following:

- finite path extent in the (κ,ω) plane,
- $\phi(E_1)$ variation,
- off-matrix contributions to the path integral.

A more elaborate simulation is required to define completely the limits to the method.

An instrument designed to make the maximum use of this technique would probably incorporate the following features:

- a large number of scattering angles incorporating a high angular range in 2Θ and extending to low angles (2Θ= 5-150^{o}),
- the highest practicable resolution at each scattering angle,
- the highest practicable detector solid angles,
- a uniform, wide range of incident neutron energies.(eV - meV).

REFERENCES

1. R.Gordon & G.T.Herman, "Three-dimensional Reconstruction from Projections: A Review of Algorithms" Int.Rev. Cytol. 38 111 (1974)

2. R.Gordon, R.Bender & G.T.Herman, "Algebraic Reconstruction Techniques (ART) for Three-Dimensional Electron Microscopy and X-Ray Photography" J.Theor.Biol. 29 471 (1970).

3. G.T.Herman,A.Lent &S.W.Rowland, "ART: Mathematics and Applications" J.Theor.Biol. 42 1 (1973).

4. R.Gordon, "A Tutorial on ART" IEEE Trans. Nucl.Sci. NS-21 78 (1974).

5. G.N.Minerbo & J.G.Sanderson, "Reconstruction of a Source from a Few (2 or 3) projections" Los Alamos Scientific Laboratory Report LA-6747-MS (1977).

6. C.G.Windsor (p229 of) "Pulsed Neutron Scattering", Taylor & Francis, London, 1981.

7. S.W.Lovesey "Theory of Neutron Scattering from Condensed Matter" Oxford University Press, Oxford ,1984 .

Fig. 1a

L1=20 m L2 = 40 m $2\theta = 5^{o}$

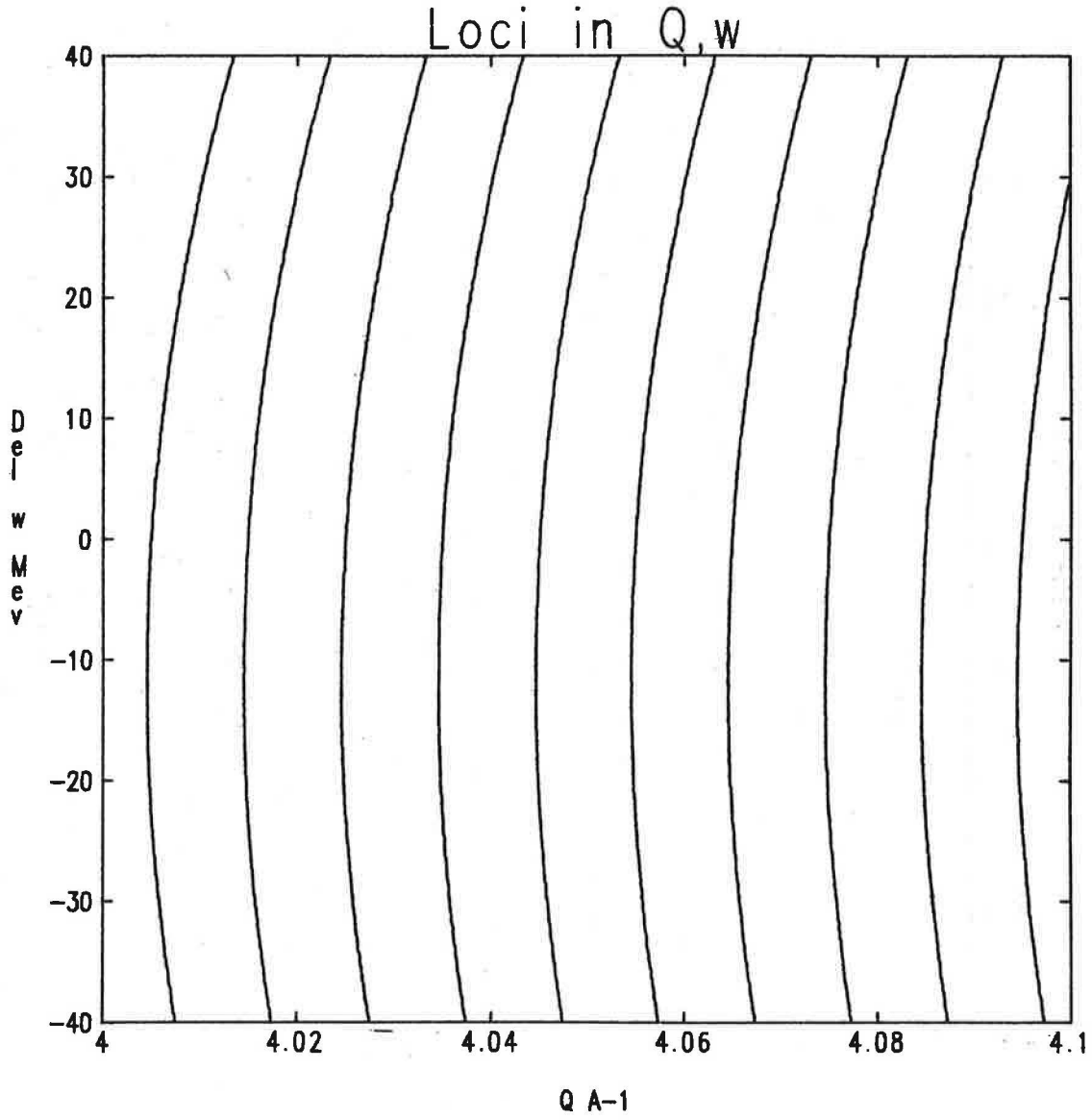

Fig. 1b

L1=20 m L2 = 20 m $2\theta = 10^{o}$

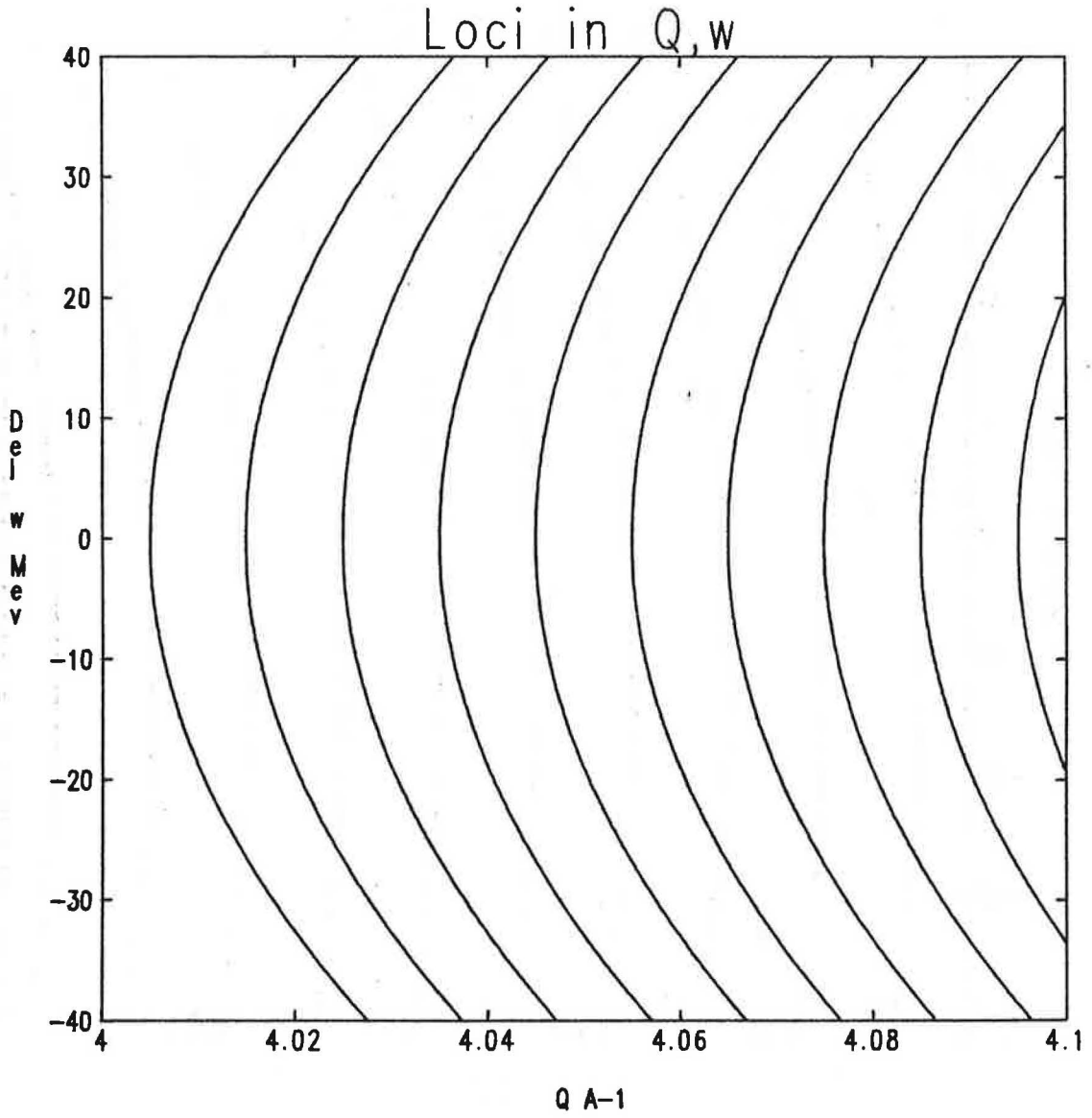

Fig. 1c

L1=20 m L2 = 10 m $2\theta = 20^{o}$

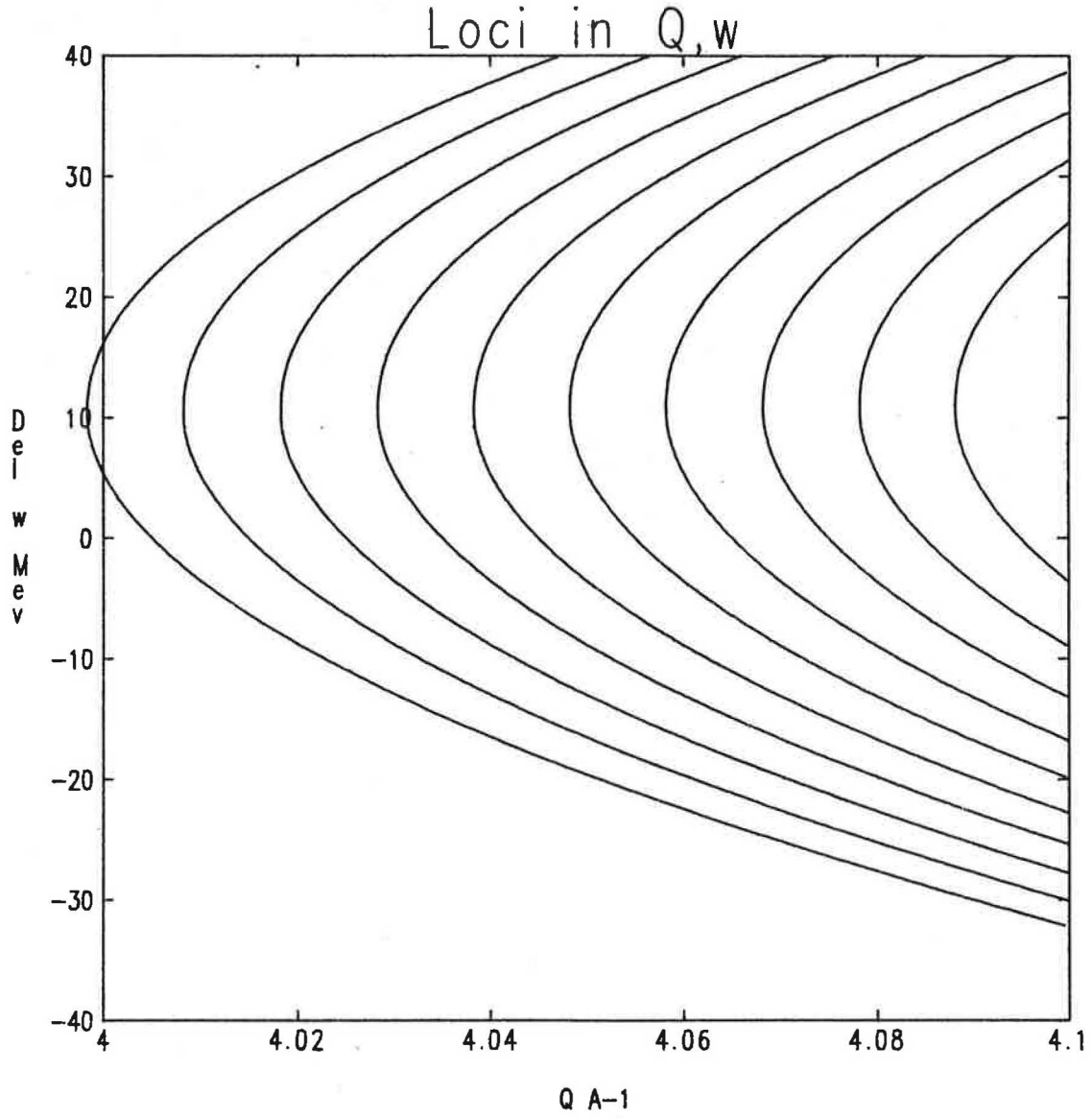

Fig. 1d

L1=20 m L2 = 5.2 m $2\theta = 40^{o}$